XI International Conference on Computational Plasticity. Fundamentals and Applications
COMPLAS XI
E. Oñate, D.R.J. Owen, D. Peric and B. Suárez (Eds)

ASSESSMENT OF THE ENHANCED ASSUMED STRAIN (EAS) AND THE ASSUMED NATURAL STRAIN (ANS) TECHNIQUES IN THE MECHANICAL BEHAVIOR OF THE SSH3D SOLID-SHELL ELEMENT

LAURENT DUCHÊNE, AMINE BEN BETTAIEB AND ANNE MARIE HABRAKEN

ARGENCO Department, MS^{2}F Division
University of Liège
Chemin des Chevreuils 1, 4000 Liège, Belgium
e-mails: {l.duchene; amine.benbettaieb; anne.habraken}@ulg.ac.be, www.argenco.ulg.ac.be

Key words: Solid-Shell finite element, Enhanced Assumed Strain technique, Assumed Natural Strain technique, Patch Test, Volumetric Locking.

1 INTRODUCTION

This paper presents the recently developed SSH3D Solid-Shell element implemented in the home-made LAGAMINE finite element code. This element is based on the Enhanced Assumed Strain (EAS) technique and the Assumed Natural Strain (ANS) technique. These techniques permit to avoid locking problems even in very bad conditions (nearly incompressible materials, very thin elements conducting to large aspect ratios, distorted element geometry…). The EAS technique artificially introduces additional degrees of freedom (DOFs) to the element. In the current configuration of the SSH3D element, up to 30 independent DOFs can be added to the 24 classical displacement DOFs (corresponding to the 3 displacements of the 8 element nodes). Contrarily to the nodal displacements, these additional DOFs are not linked between adjacent elements, so that they can be eliminated at the element level during the computation of the solution (before the assembling procedure). Nevertheless, they permit to increase the flexibility of the element which is very efficient for several locking issues. On the other hand, the ANS technique modifies the interpolation scheme for particular strain components. This technique is useful when shear and curvature locking problems are encountered. The ANS technique proved to eliminate the transverse shear locking from the element in bending dominated situations. In the current configuration of the element, four different versions of the ANS technique were implemented in the SSH3D element. Besides, a numerical integration scheme dedicated to Solid-Shell elements was implemented. It uses a user-defined number of integration points along the thickness direction, which permits to increase the element accuracy with a mesh containing a reduced number of elements along the thickness direction.

In Sections 2, 3 and 4, the main features of the SSH3D element, i.e. the EAS technique, the ANS technique and the integration scheme are briefly described. Then, in this study, the quality of the element results is assessed in different applications. The effects of the EAS technique and the integration scheme on the volumetric locking and the effects of the ANS technique on the bending behavior of the element are analyzed in Sections 5 and 6.

2 ENHANCED ASSUMED STRAIN TECHNIQUE

This section summarizes the formulation of the SSH3D Solid-Shell element. It is an 8 node hexahedral element using the Enhanced Assumed Strain (EAS) method to avoid different locking issues. The formulation of the SSH3D element departs from the Hu-Washizu variational principle:

$$\int_{\mathcal{B}} \nabla^s \underline{\eta}.\underline{\sigma} dv - G_{ext}(\underline{\eta}) = 0 \tag{1}$$

$$\int_{\mathcal{B}} \underline{\tau}.\left[\nabla^s \underline{\eta} - \underline{\varepsilon}\right] dv = 0$$

$$\int_{\mathcal{B}} \underline{\gamma}.[-\underline{\sigma} + \underline{\sigma}^m(\underline{x},\underline{q},\underline{\varepsilon})] dv = 0$$

for all variations $\underline{\eta}$, $\underline{\gamma}$, $\underline{\tau}$ of the displacement $\underline{u}$, strain $\underline{\varepsilon}$ and stress $\underline{\sigma}$ fields, respectively.

In Equation (1), the symbol ∇^s represents the symmetric gradient operator, $G_{ext}(\underline{\eta})$ is the virtual work of the external loading and $\underline{\sigma}^m(\underline{x},\underline{q},\underline{\varepsilon})$ is the stress computed by the material constitutive law at point $\underline{x}$ for the strain value $\underline{\varepsilon}$ and the current material state being represented by the vector of history variables $\underline{q}$. Note that in Equation (1), the tensors are expressed as 6 component vectors.

The main idea behind the EAS technique is the enhancement of the strain field as originally proposed by [1]:

$$\underline{\varepsilon} = \underline{\varepsilon}^{com} + \underline{\tilde{\varepsilon}} \tag{2}$$

The classical compatible part of the strain field $\underline{\varepsilon}^{com}$ is modified with the enhanced part of the strain field $\underline{\tilde{\varepsilon}}$. Note that a similar enhancement is achieved on the variation of the strain $\underline{\gamma}$. The compatible part of the strain is computed from the displacement field according to Equation (3), where the vector $\underline{U}$ contains the 24 nodal displacement DOFs and $\underline{\underline{B}}(r,s,t)$ is the classical strain-displacement operator whose components are derivatives of the shape function with respect to the spatial coordinates x, y and z. For convenience, in a finite element approach, the $\underline{\underline{B}}(r,s,t)$ matrix is expressed as a function of the intrinsic coordinates of the element r, s and t.

$$\underline{\varepsilon}^{com} = \nabla^s \underline{u} = \underline{\underline{B}}(r,s,t) \cdot \underline{U} \tag{3}$$

The enhanced part of the strain field is constructed in a similar way (see Equation (4)) using the $\underline{\underline{G}}(r,s,t)$ matrix. The additional DOFs related to the EAS techniques are included in the vector $\underline{\alpha}$.

$$\underline{\tilde{\varepsilon}} = \underline{\underline{G}}(r,s,t).\underline{\alpha} \tag{4}$$

As proposed by [1], the enhancing matrix $\underline{\underline{G}}(r,s,t)$ is build according to Equation (5) with the help of the transformation from the spatial coordinates to the intrinsic coordinates. $j(r,s,t)$ is the determinant of the Jacobian at point *(r,s,t)*, j_0 is the same at the centre of the element (defined by *r*=*s*=*t*=0). The 6 by 6 matrix $\underline{\underline{F}}_0^{-T}$ is detailed in [2]. It permits to transform a 6-component strain vector from the intrinsic coordinates to the spatial coordinates; it is computed at the centre of the element.

$$\underline{\underline{G}}(r,s,t) = \frac{j_0}{j(r,s,t)}.\underline{\underline{F}}_0^{-T}.\underline{\underline{M}}(r,s,t) \tag{5}$$

The enhancing modes of the EAS technique are included in the $\underline{\underline{M}}(r,s,t)$ matrix. Thanks to the transformation shown in Equation (5), the EAS modes are expressed in the intrinsic coordinate system in a form which is independent of the element spatial configuration, i.e., in accordance with the notation and the numbering of [3]:

$$\underline{\underline{M}}(r,s,t) = \tag{6}$$

r	0	0	0	0	0	0	0	0	0	0	0	0	0	0	*rs*	*rt*	0	0	0	0	0	0	0	*rst*	0	0	0	0	0
0	*s*	0	0	0	0	0	0	0	0	0	0	0	0	0	0	0	*rs*	*st*	0	0	0	0	0	0	*rst*	0	0	0	0
0	0	*t*	0	0	0	0	0	0	0	0	0	0	0	0	0	0	0	0	*rt*	*st*	0	0	0	0	0	*rst*	0	0	0
0	0	0	*r*	*s*	0	0	0	0	*rt*	*st*	0	0	0	0	0	0	0	0	0	0	*rs*	0	0	0	0	0	*rst*	0	0
0	0	0	0	0	*r*	*t*	0	0	0	0	*rs*	*st*	0	0	0	0	0	0	0	0	0	*rt*	0	0	0	0	0	*rst*	0
0	0	0	0	0	0	0	*s*	*t*	0	0	0	0	*rs*	*rt*	0	0	0	0	0	0	0	0	*st*	0	0	0	0	0	*rst*
1	2	3	4	5	6	7	8	9	10	11	12	13	14	15	16	17	18	19	20	21	22	23	24	25	26	27	28	29	30

This $\underline{\underline{M}}(r,s,t)$ matrix contains 30 potential EAS modes (the columns of $\underline{\underline{M}}(r,s,t)$ numbered form 1 to 30), which correspond to 30 additional DOFs. They are grouped by 3 or 6 modes corresponding to similar modes along different directions (the light and dark gray zones). The six lines of the $\underline{\underline{M}}(r,s,t)$ matrix correspond to the six components (respectively 11, 22, 33, 12, 13, 23) of the strain tensor expressed as a vector. Each EAS mode permits to increase the flexibility of the element thanks to an additional deformation mode not included in the standard 24 displacement modes (the 3 displacements of the 8 element nodes). For instance, the first mode corresponds to a linear variation along the *r*-axis of the ε_{rr} component of the strain.

An important characteristic of the EAS technique is that the additional DOFs (the $\underline{\alpha}$ values) are eliminated at the element level by static condensation before the assembling procedure of the FE code. Therefore, they do not contribute to the size of the global stiffness

matrix of the finite element technique but they improve its quality by bringing their effect on the enhanced flexibility of each SSH3D element (see [1] for further details).

In the SSH3D element, the number and the choice of the EAS modes is left to the finite element code user. The effect of the number of EAS modes on the mechanical behavior of the element is presented in Section 5.

3 THE ASSUMED NATURAL STRAIN TECHNIQUE

The Assumed Natural Strain (ANS) technique permits to avoid several locking issues by modifying the interpolation of the strain components in the element as briefly explained hereafter. Classically, the strain is computed at the integration point or at any location inside the finite element from the nodal displacements with the $\underline{\underline{B}}(r,s,t)$ matrix according to Equation (3). For some particular cases, this usual technique yields to inadequate strain values for some components depending on the location where the strain is computed. The ANS technique, originally proposed by [4] for shell elements, suggests to achieve the interpolation of the problematic strain components in two steps. First, these strain components are evaluated by the classical interpolation method at the so-called 'sampling points', where the erroneous values are not likely to be encountered. In a second step, these strain components are interpolated linearly from the sampling points to the integration points (or any location in the element).

In order to assess the efficiency of the ANS technique on the mechanical behavior of the SSH3D element, four different versions of the ANS interpolation have been implemented to date. These versions are detailed below.

For the first version [4-6], the location of the sampling points are shown in Figure 1 (a) for the 13-component (with respect to the *r*, *s*, *t* reference frame) and in Figure 1 (b) for the 23-component. The corresponding interpolation scheme is expressed by Equations (7) and (8) for the 13 and 23-components respectively. For this first version, the four other components of the strain tensor (namely 11, 22, 33, 12) are not altered by the ANS technique.

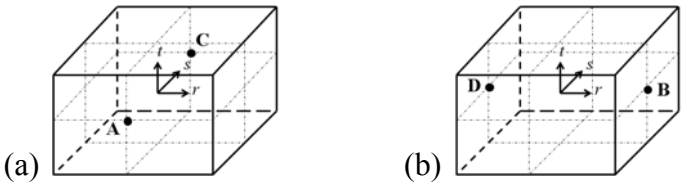

Figure 1: ANS method in the SSH3D element, version 1. Sampling points for the components 13 (a) and 23 (b).

$$E_{13}^{ANS1} = \frac{1}{2}.(1-s).E_{13}^{com}\Big|_A + \frac{1}{2}.(1+s).E_{13}^{com}\Big|_C \tag{7}$$

$$E_{23}^{ANS1} = \frac{1}{2}.(1-r).E_{23}^{com}\Big|_D + \frac{1}{2}.(1+r).E_{23}^{com}\Big|_B \tag{8}$$

It must be noted here that the ANS technique must be applied to the components of the strain expressed in the *r*, *s*, *t* reference frame and not the *x*, *y*, *z* frame of the finite element code. This is emphasized by the use of E for the strain components instead of ε in Equations

(7) and (8). The transformation tools already used for the EAS technique (see for instance Equation (5)) are adapted for the transformation of the strain tensors from the intrinsic reference frame to the global reference frame according to Equation (9).

$$\underline{\varepsilon} = \frac{j_0}{j(r,s,t)} . \underline{\underline{F}}_0^{-T} . \underline{E} \tag{9}$$

For the second ANS version of the SSH3D element [7, 8], the 33-component is also taken into consideration as shown by Figure 2 and Equations (10), (11) and (12).

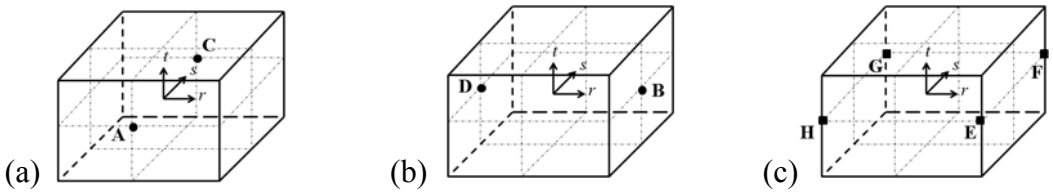

Figure 2: ANS method in the SSH3D element, version 2. Sampling points for the components 13 (a), 23 (b) and 33 (c).

$$E_{13}^{ANS2} = \frac{1}{2}.(1-s).E_{13}^{com}\Big|_A + \frac{1}{2}.(1+s).E_{13}^{com}\Big|_C \tag{10}$$

$$E_{23}^{ANS2} = \frac{1}{2}.(1-r).E_{23}^{com}\Big|_D + \frac{1}{2}.(1+r).E_{23}^{com}\Big|_B \tag{11}$$

$$E_{33}^{ANS2} = \frac{1}{4}.(1-r).(1-s).E_{33}^{com}\Big|_H + \frac{1}{4}.(1+r).(1-s).E_{33}^{com}\Big|_E + \frac{1}{4}.(1+r).(1+s).E_{33}^{com}\Big|_F + \frac{1}{4}.(1-r).(1+s).E_{33}^{com}\Big|_G \tag{12}$$

For the third version of the ANS [9, 10], the 13 and 23-component interpolation schemes are modified from the previous case by using four sampling points instead of two, as shown in Figure 3 and Equations (13), (14) and (15).

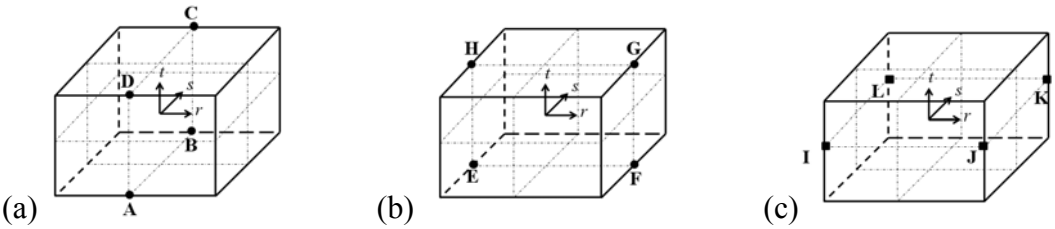

Figure 3: ANS method in the SSH3D element, version 3. Sampling points for the components 13 (a), 23 (b) and 33 (c).

$$E_{13}^{ANS3} = \frac{1}{4}.(1-s).(1-t).E_{13}^{com}\Big|_A + \frac{1}{4}.(1+s).(1-t).E_{13}^{com}\Big|_B + \frac{1}{4}.(1+s).(1+t).E_{13}^{com}\Big|_C + \frac{1}{4}.(1-s).(1+t).E_{13}^{com}\Big|_D \tag{13}$$

$$E_{23}^{ANS3} = \frac{1}{4}.(1-r).(1-t).E_{23}^{com}\Big|_E + \frac{1}{4}.(1+r).(1-t).E_{23}^{com}\Big|_F + \frac{1}{4}.(1+r).(1+t).E_{23}^{com}\Big|_G + \frac{1}{4}.(1-r).(1+t).E_{23}^{com}\Big|_H \tag{14}$$

$$E_{33}^{ANS3} = \frac{1}{4}.(1-r).(1-s).E_{33}^{com}\Big|_I + \frac{1}{4}.(1+r).(1-s).E_{33}^{com}\Big|_J + \frac{1}{4}.(1+r).(1+s).E_{33}^{com}\Big|_K + \frac{1}{4}.(1-r).(1+s).E_{33}^{com}\Big|_L \tag{15}$$

Finally, the fourth ANS version, originally proposed in this paper, uses four common sampling points for the three strain components as illustrated in Figure 4 and Equations (16), (17) and (18).

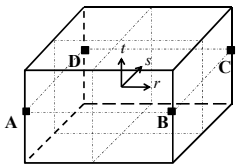

Figure 4: ANS method in the SSH3D element, version 4. Sampling points for the components 13, 23 and 33.

$$E_{13}^{ANS4} = \frac{1}{4}.(1-r).(1-s).E_{13}^{com}\Big|_A + \frac{1}{4}.(1+r).(1-s).E_{13}^{com}\Big|_B + \frac{1}{4}.(1+r).(1+s).E_{13}^{com}\Big|_C + \frac{1}{4}.(1-r).(1+s).E_{13}^{com}\Big|_D \quad (16)$$

$$E_{23}^{ANS4} = \frac{1}{4}.(1-r).(1-s).E_{23}^{com}\Big|_A + \frac{1}{4}.(1+r).(1-s).E_{23}^{com}\Big|_B + \frac{1}{4}.(1+r).(1+s).E_{23}^{com}\Big|_C + \frac{1}{4}.(1-r).(1+s).E_{23}^{com}\Big|_D \quad (17)$$

$$E_{33}^{ANS4} = \frac{1}{4}.(1-r).(1-s).E_{33}^{com}\Big|_A + \frac{1}{4}.(1+r).(1-s).E_{33}^{com}\Big|_B + \frac{1}{4}.(1+r).(1+s).E_{33}^{com}\Big|_C + \frac{1}{4}.(1-r).(1+s).E_{33}^{com}\Big|_D \quad (18)$$

4 THE INTEGRATION SCHEME OF THE SSH3D ELEMENT

An important characteristic of a finite element is the numerical integration scheme. The number and the location of the Gauss points inside the element can have a significant influence on its mechanical behavior. For instance, the reduced integration or the selective reduced integration schemes are often used to avoid volumetric locking issues for hexahedral elements with an isochoric or nearly isochoric material behavior.

In the development of a Solid-Shell element dedicated to the modeling of thin-walled structures, an improved integration scheme with a large number of integration points along the thickness direction was considered. It is indeed expected that a high gradient of stress and strain along the thickness direction is present during the deformation of thin materials (during e.g. a bending deformation mode). The classical full integration of brick elements (with two integration points along each direction) is not able to accurately capture such large gradients. In this respect, in the SSH3D element, the stress is computed along a user-defined number (ranging from 2 to 10) of integration points along the thickness direction (*t* axis), as shown in Figure 5.

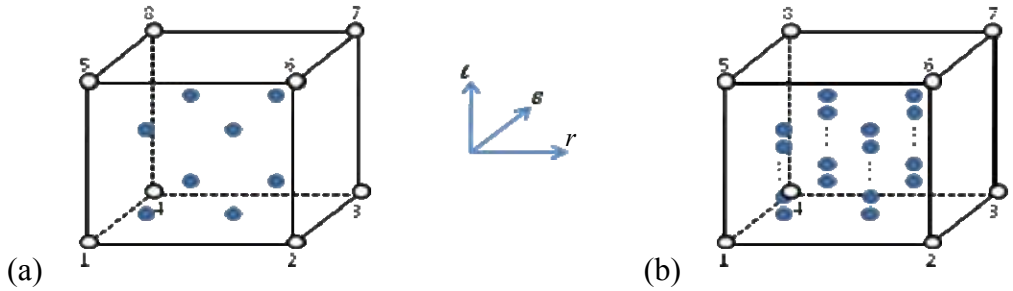

Figure 5: Integration scheme: (a) Classical full integration, (b) SSH3D integration scheme with *n* Gauss points along the thickness direction.

5 EFFECT OF EAS ON THE VOLUMETRIC LOCKING

The volumetric locking is an important issue in finite element approaches. It is likely to appear when incompressibility or nearly incompressibility is imposed by the material model (e.g. in elasticity when the Poisson's ratio approaches 0.5 or in elasto-plastic simulations where the classical assumption of plastic incompressibility is employed). Thanks to a subspace analysis, it has been shown in [11] that any deformation mode with an incompressibility constraint can be obtained as a combination of 23 linearly independent deformation modes. Consequently, an hexahedral element should be able to reproduce (without locking) these 23 modes in order to avoid volumetric locking for any deformation mode (see also [2]). As illustrated in Figure 6, these 23 modes can be divided into four groups: 12 modes corresponding to the translation of one edge of the element (Figure 6 (a)), 5 modes representing the contraction-expansion of one face (Figure 6 (b)), 3 modes related to the so-called hourglass deformation modes, where the element gets a trapezoidal shape (Figure 6 (c)) and 3 warp modes (Figure 6 (d)).

In this respect, in order to check volumetric locking issues with the SSH3D element, the deformation modes of Figure 6 are analyzed in this section for different numbers of EAS modes and different numbers of integration points along the thickness. In this study, the influence of the EAS modes is assessed by increasing successively their number according to the groups defined by the light and dark gray zones of Equation (6). Therefore, in the results, 'SSH3D - 3' means the SSH3D element with the three first EAS modes, 'SSH3D - 9' corresponds to the nine first EAS modes and so on up to 'SSH3D - 30'. The ANS technique was turned off in this section and three different integration schemes were tested with 2 (classical full integration), 5 and 8 Gauss points along the thickness direction. The incompressibility constraint was imposed by an elastic material with a Poisson's ratio close to 0.5, i.e. 0.499.

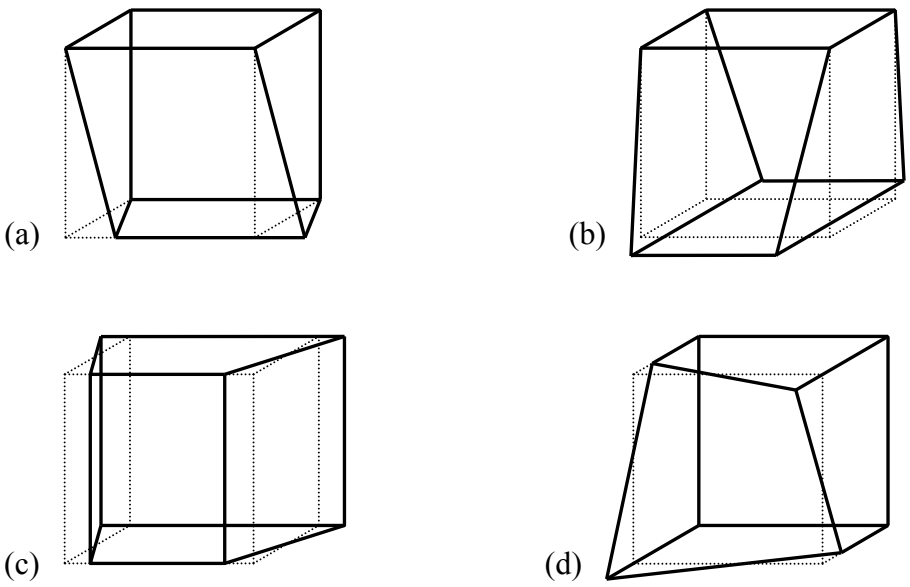

Figure 6: Groups of isochoric deformation modes: (a) Edge translation, (b) Contraction-expansion of one face, (c) Hourglass mode, (d) Warp mode.

The nodal forces required to enforce the deformation modes of Figure 6 are plotted in Figure 7, Figure 8, Figure 9 and Figure 10 for the four groups of deformation modes respectively (the nodes with non zero imposed displacement are analyzed). As they depend on the geometry of the element, the stiffness of the selected material constitutive law, the nodal forces should be regarded as arbitrary values. The purpose of the following figures is only to compare the results according to the number of EAS modes and the selected integration scheme in order to detect volumetric locking issues.

The first group of deformation modes of Figure 6 (a) is analyzed in Figure 7, where it appears that the EAS technique has almost no effect on the nodal forces. In fact, it is expected that even a classical displacement based hexahedral element with a full integration scheme will not show volumetric locking problems in this case. Indeed, this mode induces shear type deformation in the whole finite element corresponding to no volume variation, which is in accordance with the isochoric material model. Therefore, no volumetric locking is detected in this case. Anyway, a small effect of the integration scheme can be noticed.

The second group, corresponding to the contraction-expansion of one face, is treated in Figure 8. For the integration scheme with 2 Gauss points along the thickness direction (classical full integration), as in the previous case, the number of EAS modes do not influence the results. Contrarily, for the integration schemes with 5 and especially with 8 Gauss points along the thickness direction, a stiffer behavior is observed for the lowest numbers of EAS modes. For these integration schemes, volumetric locking, with a rather limited effect, is then observed when the number of EAS modes is lower than or equal to 21. The effect of the number of Gauss points on the element response is related to the fact that the volumetric constraints are applied at the Gauss points through the nearly isochoric material model.

In Figure 9, a non-zero but limited effect of the number of EAS modes can be observed. The influence of the integration scheme for the case 'SSH3D - 24' was not expected and remains unexplained.

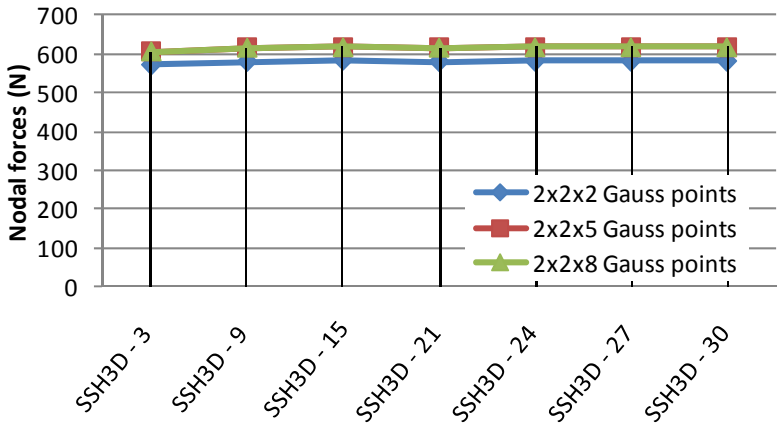

Figure 7: Nodal forces for the isochoric deformation mode of Figure 6 (a) (edge translation) versus the number of EAS modes in the SSH3D element for three different integration schemes.

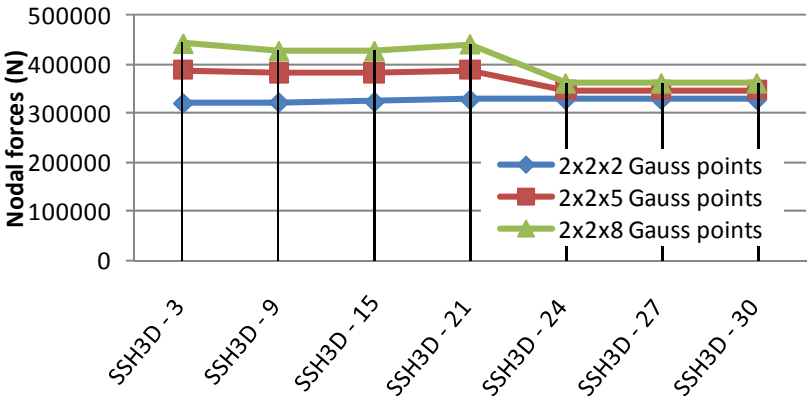

Figure 8: Nodal forces for the isochoric deformation mode of Figure 6 (b) (contraction-expansion of one face) versus the number of EAS modes in the SSH3D element for three different integration schemes.

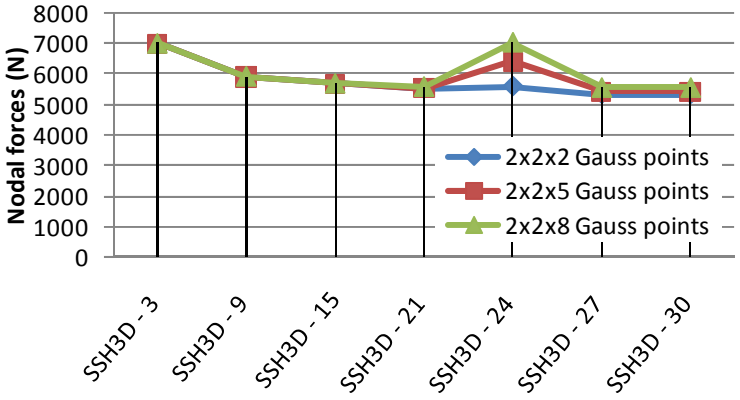

Figure 9: Nodal forces for the isochoric deformation mode of Figure 6 (c) (hourglass mode) versus the number of EAS modes in the SSH3D element for three different integration schemes.

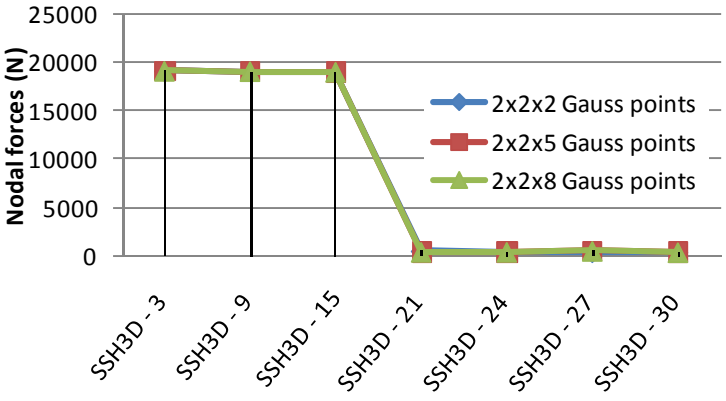

Figure 10: Nodal forces for the isochoric deformation mode of Figure 6 (d) (warp mode) versus the number of EAS modes in the SSH3D element for three different integration schemes.

The fourth group of deformation modes (Figure 6 (d)) related to the warp element shape clearly proves the occurrence of volumetric locking (see Figure 10). When the number of EAS modes is lower than or equal to 15, the computed nodal forces are much too large due to an erroneously overestimated stiffness of the element. When 21 or more EAS modes are used, the volumetric locking is avoided and the stiffness of the element abruptly drops to an accurate value. In this case, no noticeable effect of the integration scheme was observed.

6 EFFECT OF ANS ON THE BENDING BEHAVIOR OF SSH3D

In order to assess the effect of the ANS technique on the mechanical behavior of the SSH3D element, a cylindrical bending patch was investigated. The thin plate submitted to bending had the dimensions 3 x 3 x 0.02 (without units) as shown in Figure 11. The plate was fixed along the X and Z directions on its left face defined by the equation *x=0* (nodes 1, 4, 5 and 8). It was submitted to a bending loading on its right face defined by *x=3* (nodes 13, 14, 15 and 16). The imposed displacements on the right face was such that the plate was deformed into a part of a cylinder whose axis was parallel to the Y-axis and whose radius was 1000.

The accuracy of the element bending behavior is assessed by analyzing the agreement of the displacements of the free interior nodes (2, 3, 6, 7, 9, 10, 11 and 12) with the imposed cylindrical shape. In this respect, the irregular mesh presented in Figure 11 was used. The four versions of the ANS technique implemented in the SSH3D element (see Section 3) as well as the element without the ANS technique were tested.

The results are shown in Table 1, where the nodal displacements along the X and the Z axes are compared with the theoretical displacements required to obtain a perfectly cylindrical deformed geometry. It appears that the bending behavior of the SSH3D element without the ANS technique is not satisfactory (relative error of the nodal displacements up to 49%). The ANS technique with the versions 1, 2 and 3 provides even worse results with relative errors around 96%. Fortunately, the fourth version of ANS seems to be well adapted to the modeling of this bending situation. The maximum relative error on the nodal displacements is limited to 2.9% with the ANS 4, which is acceptable.

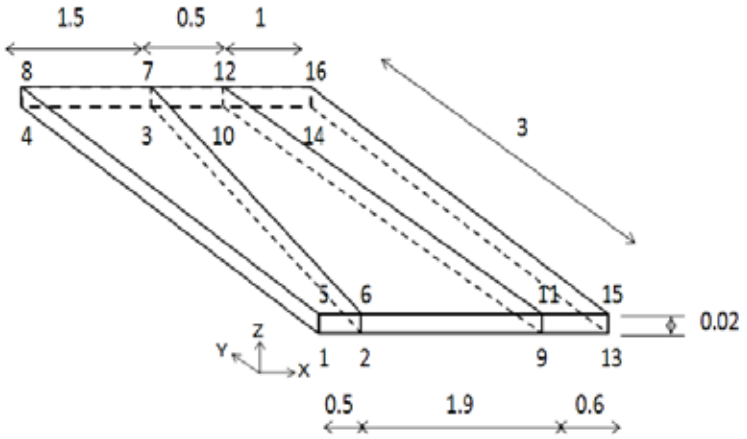

Figure 11: Geometry and irregular mesh used for the cylindrical bending patch test.

Table 1: Cylindrical bending patch test: errors from theoretical values (the largest values among the different nodes are in bold).

	Relative error on nodal displacements along X-axis (%)					Relative error on nodal displacements along Z-axis (%)				
Node	No ANS	ANS 1	ANS 2	ANS 3	ANS 4	No ANS	ANS 1	ANS 2	ANS 3	ANS 4
2	16	73	73	73	2.1	**49**	74	74	74	0.21
3	6.7	77	77	77	**2.9**	1.7	**83**	**83**	**83**	**2.3**
6	**18**	73	73	73	1.7	**49**	74	74	74	0.20
7	4.7	88	88	88	1.6	1.7	**83**	**83**	**83**	**2.3**
9	3.7	17	17	17	0.24	0.35	3.6	3.6	3.6	0.010
10	6.3	**97**	**96**	**96**	2.3	2.0	41	41	41	1.1
11	3.1	13	13	13	0.13	0.35	3.6	3.6	3.6	0.011
12	4.8	71	71	71	2.2	2.0	41	41	41	1.1

7 CONCLUSIONS

This paper presents the main features of the recently developed SSH3D Solid-Shell element. They have been implemented in order to improve the mechanical behavior of the element in various applications dedicated to Solid-Shell or shell elements, e.g. thin-walled structures submitted to large strains and large displacements. These features are:

- The EAS technique which improves the flexibility of the element thanks to additional degrees of freedom. In the SSH3D element, the finite element user can choose which EAS modes (from 1 to 30) he wants to employ according to its particular application.
- The ANS technique which modifies the interpolation of the strain tensor in order to circumvent several locking issues, e.g. transverse shear locking in bending dominated problems or curvature locking. Four different versions of the ANS technique have been implemented in the SSH3D element. Among them, three have been extracted from the literature and the fourth one is an original contribution of the SSH3D element.
- An integration scheme dedicated to Solid-Shell elements. A classical full integration scheme (2 x 2 Gauss points) is employed in the plane of the element, while a user-defined number (from 2 to 10) integration points can be used along the thickness direction. This permits to capture the through-thickness stress and strain gradients with a limited number of element layers.

In this study, the influence of the EAS technique and the integration scheme on the volumetric locking and the influence of the ANS technique on the bending behavior were analyzed. The following comments were attained:

- The volumetric locking can be avoided by using at least 21 EAS modes if a 2 x 2 x 2 integration scheme is used. If 5 or 8 integration points along the thickness direction are used, 24 EAS modes are required.
- An accurate bending behavior is obtained during the cylindrical bending patch test with the fourth version of the ANS technique. The other versions as well as the element without ANS conducted to an erroneous bending behavior of the SSH3D element.

Further applications will be investigated in order to confirm or adapt the conclusions drawn in this paper.

ACKNOWLEDGEMENTS

The authors acknowledge the Interuniversity Attraction Poles Program - Belgian State – Belgian Science Policy (Contract P6/24). L.D. and A.M.H. also thank the Belgian Fund for Scientific Research FRS-FNRS for its financial support.

REFERENCES

[1] Simo, J.C. and Rifai M.S. A Class of Mixed Assumed Strain Methods and the Method of Incompatible Modes. *Int. J. Num. Meth. Engng.* (1990) **29**: 1595-1638.

[2] Alves de Sousa, R.J., Yoon, J.W., Cardoso, R.P.R., Fontes Valente, R.A., Gracio, J.J. On the use of a reduced enhanced solid-shell (RESS) element for sheet forming simulations. *Int. J. Plast.* (2007) **23**: 490-515.

[3] Andelfinger, U. and Ramm, E. EAS-elements for two-dimensional, three-dimensional, plate and shell structures and their equivalence to HR-elements. *Int. J. Num. Meth. Engng.* (1993) **36**: 1311-1337.

[4] Dvorkin, E.N. and Bathe K.-J. A continuum mechanics based four-node shell element for general nonlinear analysis. *Engineering computations* (1984) **1**: 77-88.

[5] Hauptmann, R., Schweizerhof, K. and Doll, S. Extension of the 'solid-shell' concept for application to large elastic and large elastoplastic deformations. *Int. J. Num. Meth. Engng.* (2000) **49**: 1121-1141.

[6] Nguyen, N.H. Development of solid-shell elements for large deformation simulation and springback prediction. Ph.D. Thesis (2009), University of Liège, Belgium. Available from http://bictel.ulg.ac.be/ETD-db/collection/available/ULgetd-11012009-164626/

[7] Vu-Quoc, L. and Tan, X.G. Optimal solid shells for non-linear analyses of multilayer composites. I. Statics. *Comput. Meth. Appl. Mech. Eng.* (2003) **192**: 975-1016.

[8] Klinkel, S., Gruttmann, F. and Wagner, W. A robust non-linear solid shell element based on a mixed variational formulation. *Comput. Meth. Appl. Mech. Eng.* (2006) **195**: 179-201.

[9] Schwarze, M. and Reese, S. A reduced integration solid-shell finite element based on the EAS and the ANS concept-Geometrically linear problems. *Int. J. Num. Meth. Engng.* (2009) **80**: 1322-1355.

[10] Cardoso, R.P.R., Yoon, J.W., Mahardika, M., Choudhry, S., de Sousa, R.J.A. and Fontes Valente, R.A. Enhanced assumed strain (EAS) and assumed natural strain (ANS) methods for one-point quadrature solid-shell elements. *Int. J. Num. Meth. Engng.* (2008) **75**: 156-187.

[11] Alves de Sousa, R.J., Natal Jorge, R.M., Fontes Valente, R.A., César Sá, J.M.A. A new volumetric and shear locking-free EAS element. *Engineering Computations* (2003) **20**:896-925.